# Towards Energy-Aware LoRaWAN ADR for Mobile Scenarios Through Dynamic Margin Control

**Geraldo A. Sarmento Neto**[1], **Thiago A. R. Silva**[1,2], **Pedro F. F. Abreu**[1], **Artur F. da S. Veloso**[1], **Luis H. de O. Mendes**[1], **José Valdemir R. Junior**[1]

[1]Federal University of Piauí (UFPI), Teresina – PI – Brazil

[2]Federal Institute of Maranhão (IFMA), Barra do Corda – MA – Brazil

{geraldosarmento,thiago.allisson,pedroffda

arturfdasveloso,luishenriqueom,valdemirreis}@ufpi.edu.br

***Abstract.*** *In LoRaWAN networks, the ADR mechanism plays an essential role in dynamically adjusting the data rate to optimize energy consumption and network efficiency. However, since it is not suitable for mobile environments, alternative solutions such as MB-ADR have been proposed. This study enhances the MB-ADR scheme by dynamically adjusting the ADR* $margin\_db$ *value based on SNR variability. Simulations with up to 1,000 mobile nodes demonstrate a 52.5% improvement in energy efficiency and a 42.18% reduction in latency while preserving packet delivery ratios similar to those of the fixed-margin MB-ADR. The proposed approach outperforms standard ADR in high-mobility scenarios, demonstrating its potential to enhance IoT network performance.*

## 1. Introduction

The rapid growth of Internet of Things (IoT) has transformed how devices communicate within a networked ecosystem. IoT connects billions of devices, from simple sensors to complex systems, enabling data exchange and intelligent decision-making. Low Power Wide Area Networks (LPWANs) have become key to IoT deployments, offering long-range communication with minimal energy consumption, ideal for applications requiring wide coverage and extended device operation, particularly in areas with limited power access [Janssen et al. 2023].

Among LPWANs technologies, Long Range Wide Area Network (LoRaWAN) stands out as a scalable protocol operating on unlicensed bands, offering cost-effective, energy-efficient long-range communication. Utilizing Long Range (LoRa) modulation, it ensures reliable low-power communication over extended distances. LoRaWAN supports large-scale deployments with end-to-end encryption and adaptive data rate management, making it ideal for smart cities, agriculture, and industrial automation [Bonilla et al. 2023]. Its open standard promotes interoperability and global adoption.

An important factor influencing LoRaWAN performance is its transmission parameters, which significantly impact network efficiency and device longevity. The Spreading Factor (SF) determines the number of chips per symbol in signal modulation and defines the trade-off between data rate and communication robustness. Transmission Power (TP) regulates the strength of the signal, affecting both range and energy consumption. Bandwidth (BW) influences the data rate and channel capacity, while the Coding Rate (CR) enhances error correction, improving resilience against interference. The proper configuration of these parameters is essential to optimize the trade-offs between communication range, reliability, and energy efficiency in LoRaWAN deployments [Janssen et al. 2023].

One of the key mechanisms in LoRaWAN for dynamic transmission parameter management is the Adaptive Data Rate (ADR) algorithm. It adjusts SF, TP, and other settings based on network conditions and device environment, using Signal-to-Noise Ratio (SNR) to evaluate link quality and optimize performance. By autonomously adapting these parameters, ADR reduces congestion, minimizes energy consumption, and supports higher device density [Kufakunesu et al. 2020]. Its impact on scalability and performance is crucial for large-scale LoRaWAN deployments.

A critical aspect of ADR is the $margin\_db$ value, an error margin accounting for optimistic channel assumptions. Typically set to 10 dB, $margin\_db$ influences network capacity, link reliability, and energy efficiency [Semtech 2016]. Increasing it reduces packet loss by favoring lower data rates, while decreasing it boosts capacity at the cost of higher packet loss. Dynamic adjustments to $margin\_db$ are essential in networks with mobile nodes [Wang et al. 2024].

In this context, this paper proposes an enhancement to the Median-Based ADR (MB-ADR) scheme presented in [Sarmento Neto et al. 2024], enabling the dynamic determination of the $margin\_db$ variable based on the variability level of SNR. The improved scheme is introduced and evaluated within a simulated environment featuring instances of 200 to 1,000 mobile nodes. Through this evaluation, the enhanced MB-ADR successfully compensated for inaccurate link quality estimates, achieving an overall improvement of 52.5% in energy efficiency compared to the original MB-ADR.

The primary contributions of this paper are threefold:

- A novel method for dynamically adjusting the $margin\_db$ value to accommodate varying levels of SNR variability in mobile scenarios;
- The development and presentation of an enhanced scheme, which incorporates significant improvement to the MB-ADR approach to achieve improved energy efficiency;
- A comprehensive performance evaluation of the enhanced scheme in simulated environments, demonstrating its benefits in large-scale deployments with mobile nodes.

The remainder of this paper is organized as follows: Section 2 reviews related work. Section 3 provides background information on LoRaWAN and the ADR mechanism. Section 4 details the proposed solution. Section 5 describes the methodology used in the study. Section 6 presents and discusses the results. Finally, Section 7 concludes the paper and highlights future directions.

## 2. Related Work

Several studies propose ADR schemes tailored for mobility [Durand et al. 2023, Farhad et al. 2023, Soy 2023]. However, many of those that rely on a representative SNR value employ the same static $margin\_db$ value as the standard ADR [Jiang et al. 2023, Moysiadis et al. 2021]. These approaches highlight the importance of optimizing the SNR evaluation process to accommodate dynamic environments and improve the adaptability of

ADR mechanisms. Table 1 lists the related work, presenting the scheme name, how the variable $margin\_db$ is adjusted, and the main method adopted by the proposed solution.

**Table 1. Summary of related work.**

| *Reference* | *Scheme name* | $margin\_bd$ *adjustment* | *Method* |
|---|---|---|---|
| [Benkahla et al. 2021] | VHMM-based E-ADR | Not used | Variable hidden Markov model |
| [de Jesus et al. 2021] | ADRx | Dynamic | Reference DER value |
| [Moysiadis et al. 2021] | LR-ADR | Static | Linear regression |
| [Durand et al. 2023] | MADERE | Static | Probability-based estimation |
| [Farhad et al. 2023] | M-ADR | Static | Kalman filter |
| [Jiang et al. 2023] | K-ADR | Static | Ordinary Kriging function |
| [Soy 2023] | Blind-ADR | Not used | Round-robin of fixed SF values |
| [Wang et al. 2024] | Mobile ADR | Dynamic | Signal characteristics and node movement data |
| This work | MB-ADR | Dynamic | Median and Interquartile Range |

Mobile ADR is a scheme proposed in [Wang et al. 2024] that stands out for its dynamic determination of the parameter $margin\_db$, adjusting the installation margin of the network to compensate for inaccurate link quality estimates. This approach ensures a more responsive adaptation to rapidly changing radio conditions. The use of Time on Air (ToA) as a criterion and the expanded bandwidth range further enhance data rates, making it particularly beneficial in dynamic environments. Nevertheless, the reliance on precise positional data of end devices for variable estimation introduces practical challenges. Such dependence on localization infrastructure or accurate positioning methods may complicate deployments in scenarios where this data is not readily available or entails additional overhead.

The authors in [de Jesus et al. 2021] build upon the existing body of research concerning the optimization of the ADR mechanism in LoRaWAN. By introducing the novel ADRx algorithm, they aim to enhance the reliability of transmission parameters by dynamically adapting the $margin\_db$ value at runtime. This approach eliminates the need for prior network knowledge, as opposed to static configurations seen in other works, and achieves improvements in both Data Extraction Rate (DER) and energy efficiency. However, the proposal is limited to the adjustment of the $margin\_db$ parameter, leaving other aspects of the ADR mechanism unchanged. As a result, the algorithm might not fully explore the potential of more comprehensive resource allocation techniques. Additionally, while the dynamic adjustment of $margin\_db$ improves adaptability, it may not address situations where the default assumptions of ADR — such as uniform traffic patterns or static device positions — are not valid.

The study by [Benkahla et al. 2021] introduces the Variable Hidden Markov Model-based Enhanced Adaptive Data Rate (VHMM-based E-ADR) algorithm, an ADR scheme designed for scenarios involving mobile nodes with unknown trajectories. This method demonstrates substantial improvements in packet loss rates and energy efficiency compared to other ADR approaches. Moreover, the research emphasizes the importance of dynamically adjusting the retransmission threshold ($m$) used on the end-device side of ADR, discussing its impact on optimizing coverage and energy consumption. The authors conclude that $m$ configurations may still require extensive calibration to ensure adaptability across diverse network conditions. This highlights a trade-off between proactive configuration adjustments and the computational cost of dynamic predictions.

## 3. Background

This section provides an overview of the concepts pertinent to this study. It covers discussions on LoRaWAN technology, followed by an exploration of the ADR mechanism and its impact on optimizing network performance.

### 3.1. LoRaWAN

LoRaWAN is a low-power, wide-area network protocol designed for IoT applications. It enables long-range communication with low power consumption, making it ideal for devices with limited battery life. Operating in unlicensed frequency bands, it supports cost-effective deployments and provides scalability and security for a variety of use cases, such as smart cities and industrial automation [Bonilla et al. 2023].

The physical layer of LoRaWAN is based on LoRa, which employs Chirp Spread Spectrum (CSS) modulation to achieve robust and long-range communication [Kufakunesu et al. 2020]. This modulation technique spreads the signal over a wider bandwidth, making it resistant to interference and enabling reception even in challenging environments. The chirp signal's inherent resilience to noise and multi-path effects makes LoRaWAN particularly advantageous for outdoor and rural deployments.

The architecture of LoRaWAN is organized into three main components: End Devices (EDs), Gateways (GWs), and a Network Server (NS) [Janssen et al. 2023]. EDs communicate with GWs, which acts as intermediaries to forward messages to the NS. This star-of-stars topology ensures efficient communication and simplifies device management. Moreover, the NS handles tasks such as message deduplication, authentication, and adaptive data rate management, ensuring reliable and optimized network performance.

LoRaWAN communication is asymmetric, with uplink (UL) transmissions from EDs to GWs occurring more frequently than downlink (DL) transmissions from GWs to EDs. This asymmetry aligns with most IoT use cases, where sensors primarily send data to the server. The protocol uses Aloha-based channel access for uplinks, while downlinks occur within predefined receive windows, ensuring synchronization and reducing energy consumption [Bonilla et al. 2023].

Transmission parameters in LoRaWAN are essential elements for balancing the trade-offs between range, data rate, and energy efficiency. The SF determines how many chips are used to represent each symbol in the signal modulation, impacting the communication robustness and data rate. TP affects signal strength, with higher values enabling longer-range communication but at the cost of increased power consumption. BW influences data rate and noise immunity, while CR provides error correction capabilities, enhancing communication reliability in noisy environments. These parameters are dynamically adjusted through the ADR mechanism to optimize network performance for diverse application requirements [Kufakunesu et al. 2020].

### 3.2. Adaptive Data Rate

ADR is a mechanism in LoRaWAN that optimizes performance by adjusting the transmission parameters of EDs based on link quality and environmental conditions [Farhad et al. 2023]. By adapting the data rate and transmission power, ADR maximizes energy efficiency and network connectivity.

The ADR algorithm uses several variables based on SNR to determine the appropriate data rate for a device. The variable $SNR_m$ represents the maximum SNR obtained from the last $M = 20$ packets received at the network server. The variable $SNR_{req}$ defines the required SNR for packet demodulation based on the current SF, while $SNR_{margin}$ specifies the minimum SNR margin needed to ensure reliable communication.

In addition to these variables, the $margin\_db$ serves as an error margin to compensate for inaccurate link quality estimates [de Jesus et al. 2021]. The variable $Steps$ enables fine-tuning of the parameters, allowing more precise control over the data rate and transmission power. These variables work together to balance communication range and energy efficiency. This scheme is summarized in a flowchart shown in Figure 1.

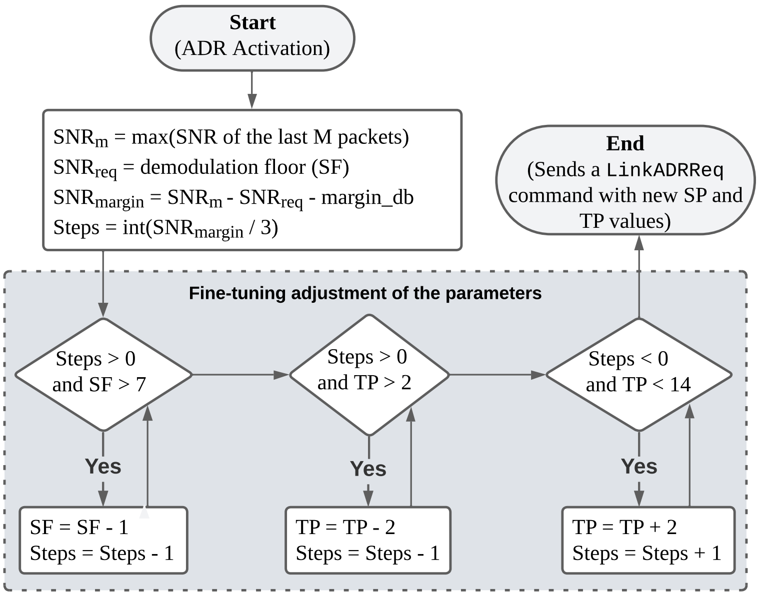


**Figure 1. ADR scheme flowchart.**

Overall, the ADR algorithm operates by evaluating the link quality between an ED and a GW and adjusting the transmission parameters accordingly. The adaptation of the SF and TP is performed based on the SNR. For instance, if the SNR value is high, indicating a strong link, the device can reduce its SF and TP, thereby saving energy. Conversely, if the link quality deteriorates, the device increases the SF and TP to ensure successful communication [Wang et al. 2024].

While effective in static or low-mobility scenarios, ADR faces challenges in highly mobile environments due to rapid link quality fluctuations [Farhad et al. 2023]. These fluctuations delay parameter updates, causing packet losses and higher energy consumption, highlighting the need for improvements to better support mobile nodes and maintain efficient communication.

# 4. Proposed Solution

This section initially describes the original MB-ADR scheme and its guiding principles. It then presents the enhanced MB-ADR scheme with the adjustment method for dynamic margin control.

## 4.1. Median as a Representative Estimator of SNR

As mentioned earlier, the standard ADR algorithm estimates signal quality using the $SNR_m$ variable, as outlined in Figure 1. However, in dynamic environments where channel conditions fluctuate frequently, metrics such as maximum or mean SNR values often fail to provide accurate estimates [Sarmento Neto et al. 2024], which can lead to suboptimal transmission parameter adjustments.

To address these challenges, it is essential to analyze the data distribution. In this context, a distribution of 25,000 sets, each containing $M = 20$ SNR values, totaling 500,000 samples, was collected using the ADR mechanism in a simulated network with 500 mobile end devices. The parameters used were similar to those described in Section 5. The histogram of these samples, shown in Figure 2(a), reveals an asymmetric distribution, with a higher concentration of data points at the lower end of the x-axis. Furthermore, an analysis of 15 randomly selected box plots from the 25,000 sets confirms the skewed nature of the distribution, primarily due to significant SNR variability and numerous outliers, as shown in Figure 2(b).

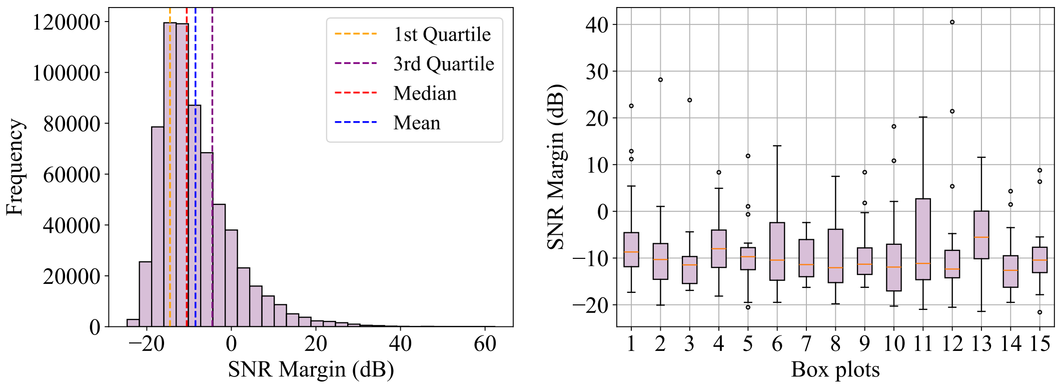


(a) (b)

**Figure 2. Distribution of SNR values using a (a) histogram and (b) box plots.**

Assuming a skewed SNR distribution, using the maximum or mean value does not adequately represent the data [Duan et al. 2021]. In this context, MB-ADR was proposed as an alternative to ADR, using the median as a more effective measure in mobile environments [Sarmento Neto et al. 2024]. The scheme also employs the InterQuartile Range (IQR) method to exclude outliers [Perez and Tah 2020], ensuring that extreme values do not distort the $SNR_m$ assignment. This minimizes the impact of fluctuations and enables more stable parameter adjustments in ADR.

## 4.2. Enhancing MB-ADR with a Dynamic $margin\_db$ Value

Despite the promising performance of MB-ADR in [Sarmento Neto et al. 2024], its fixed $margin\_db$ value is inadequate for environments with high mobility. As devices move faster, channel conditions fluctuate rapidly, making a static $margin\_db$ unsuitable for defining an adequate margin [Wang et al. 2024].

Based on this premise, an enhanced MB-ADR scheme is proposed, implemented at the server level, which incorporates a dynamic estimation method for $margin\_db$ based on SNR variability. For this purpose, it is necessary to previously determine $SNRvar_{max}$ and $SNRvar_{min}$, representing the maximum and minimum variability values of a significant network sample containing $N$ elements, similar to the one analyzed in Section 4.1 for observing data distribution. The variables $SNRvar_{max}$ and $SNRvar_{min}$, formalized in Equations 1 and 2, respectively, are employed by the proposed scheme as thresholds to define the extreme values of $margin\_db$.

$$SNRvar_{max} = \max\left(|x_{i+1} - x_i|\right) \quad \text{for} \quad i = 1, 2, \ldots, n-1 \tag{1}$$

$$SNRvar_{min} = \min\left(|x_{i+1} - x_i|\right) \quad \text{for} \quad i = 1, 2, \ldots, n-1 \tag{2}$$

At each activation of the proposed ADR, a set $SNRlist = \{s_1, s_2, \ldots, s_M\}$ is generated, containing the last $M$ SNR values collected from a single end device. The variable $SampleVar$ is subsequently defined to store the average variability of the sample contained in $SNRlist$, as expressed in Equation 3.

$$SampleVar = \frac{\sum_{i=1}^{M-1} |s_{i+1} - s_i|}{M-1} \tag{3}$$

Once these variables are established, the dynamic value of $margin\_db$ is determined using linear interpolation to identify the most suitable error margin based on the average variability of the current sample. This step is formalized as:

$$margin\_db = \begin{cases} marg_{max}, & \text{if } SampleVar \geq SNRvar_{max}, \\ marg_{min}, & \text{if } SampleVar \leq SNRvar_{min}, \\ marg_{max} - \Big\lfloor \frac{SampleVar - SNRvar_{min}}{SNRvar_{max} - SNRvar_{min}} & \\ \quad \cdot (marg_{max} - marg_{min}) \Big\rfloor, & \text{otherwise.} \end{cases} \tag{4}$$

where $marg_{min}$ and $marg_{max}$ represent the extreme values of $margin\_db$: 5 dB and 15 dB, respectively [de Jesus et al. 2021, Wang et al. 2024]. The linear interpolation was chosen for its suitability in handling the gradual variation of $SampleVar$, ensuring a continuous transition between the limits $marg_{max}$ and $marg_{min}$, and for its low computational complexity, contributing to a faster response [Ouermi et al. 2024].

Following the outlined principles of the proposed method, the steps of enhanced MB-ADR are detailed in Algorithm 1. First, $SampleVar$ is computed from $SNR_{list}$ in lines 1-2, with the $getMeanVariability$ function simplifying the process defined in Equation 3. Lines 3-8 perform the linear interpolation as described in Equation 4 to compute the dynamic $margin\_db$. Finally, lines 9-10 apply the MB-ADR strategy to obtain $SNR_m$, as described in Section 4.1, and guide the algorithm through the standard ADR steps, which are described in lines 11-23.

**Algorithm 1:** Enhanced MB-ADR Algorithm

**Input:** $SF = 7 \sim 12,\ TP = 2 \sim 14,\ SNRvar_{min},\ SNRvar_{max},$
$marg_{min} = 4,\ marg_{max} = 16,\ M = 20$

$SNRlist \leftarrow getLastULpackets(M)$
$SampleVar = getMeanVariability(SNRlist)$
**if** $SampleVar >= SNRvar_{max}$ **then**
    $margin\_db \leftarrow marg_{max}$
**else if** $SampleVar <= SNRvar_{min}$ **then**
    $margin\_db \leftarrow marg_{min}$
**else**
    $margin\_db \leftarrow marg_{max} - \lfloor (SampleVar - SNRvar_{min})/(SNRvar_{max} - SNRvar_{min}) * (marg_{max} - marg_{min}) \rfloor$
$SNRlist.removeOutliers()$
$SNR_m \leftarrow getMedian(SNRlist)$
$SNR_{req} \leftarrow demodulationFloor(current\ data\ rate)$
$SNR_{margin} \leftarrow SNR_m - SNR_{req} - margin\_db$
$Steps \leftarrow int\ (SNR_{margin}/3)$
**while** $Steps > 0\ \ and\ \ SF > SF_{min}$ **do**
    $SF \leftarrow SF - 1$
    $Steps \leftarrow Steps - 1$
**while** $Steps > 0\ \ and\ \ TP > TP_{min}$ **do**
    $TP \leftarrow TP - 2$
    $Steps \leftarrow Steps - 1$
**while** $Steps < 0\ \ and\ \ TP < TP_{max}$ **do**
    $TP \leftarrow TP + 2$
    $Steps \leftarrow Steps + 1$
NS sends $LinkADRReq(SF,\ TP)$

## 5. Methodology

This section outlines the methodology employed in this study, encompassing the simulation environment and the parameterization used. Finally, the metrics adopted for the analysis of the proposed scenario are presented.

### 5.1. Simulation Setup

To evaluate the performance improvements of the MB-ADR scheme compared to its original version and the standard ADR, simulation scripts were developed in C++ and executed in Network Simulator 3 (NS-3)[1]. The simulations utilized a widely adopted LoRaWAN module [Farhad et al. 2023, Kufakunesu et al. 2022] provided by SIGNET[2].

In the simulations, 200 to 1,000 LoRa end devices were randomly deployed in a 10 km × 10 km area, transmitting 144 packets over 24 hours, representing a pet tracking application [Anwar et al. 2021]. Each simulation was repeated 10 times with different

[1] https://www.nsnam.org/releases/ns-3-42
[2] https://github.com/signetlabdei/lorawan

random seeds to ensure robustness, with results analyzed using a 95% confidence interval to assess the data variability and ensure the reliability of the conclusions.

To represent a more realistic channel, the Log-distance path loss model [de Jesus et al. 2021] was employed. Additionally, shadowing effects were simulated by incorporating stochastic signal variations caused by obstacles and environmental reflections [Moysiadis et al. 2021]. A combined propagation loss and shadowing model is defined as:

$$L(d) = L(d_0) + 10\gamma \log_{10}\left(\frac{d}{d_0}\right) + X_\sigma \tag{5}$$

where $L(d)$ represents the path loss in decibels (dB) at a distance $d$ from the transmitter, $L(d_0)$ is the path loss measured at a reference distance $d_0$, $\gamma$ is the path loss exponent, and $X_\sigma$ represents shadowing, modeled as a normally distributed variable with a mean of zero and a standard deviation $\sigma$. Table 2 summarizes the parameters used in this work and their respective values.

The mobility of the EDs was included with the aid of the Random Walk model [Sarmento Neto et al. 2024], allowing random movement where the direction and speed of each node are redefined at regular time intervals. To represent varying mobility levels, five distinct speed categories were established, each associated with a specific movement pattern [Teymuri et al. 2023]:

- *Class 1: 0.1 to 4 m/s*: Pedestrians in urban and rural environments, motorized wheelchairs, and low-mobility activities [Nico and Punch 2019];
- *Class 2: 4 to 8 m/s*: Urban cyclists, electric scooters, and slow-moving delivery vehicles [Ren et al. 2022];
- *Class 3: 8 to 12 m/s*: Road cyclists, small electric cars, and motorcycles in light traffic conditions [El Chall et al. 2019];
- *Class 4: 12 to 16 m/s*: Vehicles in moderate traffic on urban and suburban roads and highways [Ferrari et al. 2020];
- *Class 5: 16 to 20 m/s*: Vehicles on highways and high-speed intercity roads [Di Renzone et al. 2024].

### 5.2. Employed Metrics

To analyze the results, key performance metrics were used, including Packet Delivery Ratio (PDR), energy efficiency, and latency, providing insights into reliability, energy consumption, and channel conditions. The PDR, defined in Equation 6, is the ratio of packets successfully received by the GW to those sent by the ED. It measures communication reliability and reflects network transmission effectiveness [Teymuri et al. 2023] and can be defined as:

$$PDR = \frac{N_{received}}{N_{sent}} \tag{6}$$

where $N_{received}$ denotes the total number of packets successfully received by the GW, and $N_{sent}$ represents the total number of packets transmitted by all EDs.

**Table 2. Parameterization employed.**

| *Simulation Parameter* | *Value* |
|---|---|
| Area dimensions | 10 km x 10 km |
| Number of EDs | [200, 1000] |
| Packet rate | 144 packets/day |
| Simulation time | 24 hours |
| Packet size | 30 bytes |
| UL packet transmission limit | 8 |
| Mobility model | 2D Random Walk |
| ED movement speed | [0.1 , 20.0] m/s |
| Path loss exponent ($\gamma$) | 3.76 |
| Carrier frequency | 868 MHz (EU-868) |
| Bandwidth | 125 KHz |
| Coding rate | 4/8 |

The energy efficiency ($EE$) measures the successfully transmitted data (bits) per energy consumed (J), reflecting the device communication efficiency [Al-Gumaei et al. 2022]. It is calculated as:

$$EE = \frac{N_{bits}}{E} \tag{7}$$

where $N_{bits}$ refers to the total number of bits successfully received by the GW, and $E$ represents the total energy consumed by all EDs.

Finally, the latency ($\bar{\Delta}$) measures the mean delay between the transmission and reception of packets successfully received in the network. For each packet $i$, the latency $\Delta_i$ is the shortest time difference between its transmission, $T^{(i)}_{\text{send}}$, and reception, $T^{(i,j)}_{\text{recv}}$, across all receivers $j \in \mathcal{R}_i$ that received the packet. It is calculated as:

$$\bar{\Delta} = \frac{1}{N_{\text{received}}} \sum_{i=1}^{N_{\text{sent}}} \min_{j \in \mathcal{R}_i} \left( T^{(i,j)}_{\text{recv}} - T^{(i)}_{\text{send}} \right) \tag{8}$$

where $\mathcal{R}_i$ is the set of receivers of packet $i$. This metric captures the average end-to-end delay, combining propagation and processing times.

## 6. Results

To evaluate the proposed scheme, the speed classes presented in Subsection 5.1 were varied while maintaining a fixed number of 500 end devices. As shown in Figure 3(a), the PDR of enhanced MB-ADR (with dynamic $margin\_db$) is lower than original MB-ADR (with fixed $margin\_db$) in the first three speed classes. However, from 12 m/s to 20 m/s, both schemes show similar PDR values around 0.75, while standard ADR drops significantly, with PDR values below 0.3 starting from the second speed class.

From the perspective of average energy efficiency, the enhanced MB-ADR outperforms from the first speed class and further extends its advantage over the other schemes in subsequent speed classes, as depicted in Figure 3(b). It achieves an overall improvement of approximately 50.3% and 85.16% compared to the original MB-ADR and standard ADR, respectively.

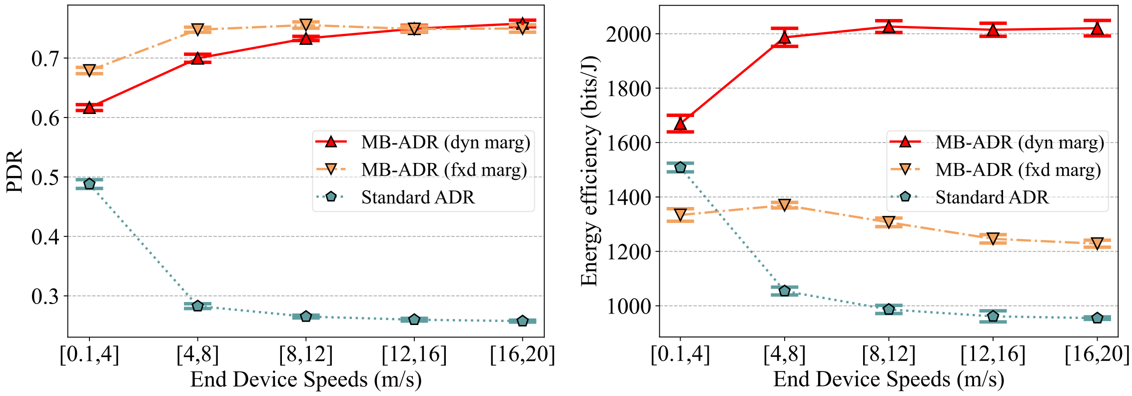


(a) (b)

**Figure 3. Network performance for different speed classes in terms of average (a) PDR and (b) energy efficiency.**

To analyze the performance of the enhanced MB-ADR in greater detail, Figure 4 presents the results of a scenario subset, varying the number of EDs and employing speeds between 12 m/s and 20 m/s, which corresponds to the range where the proposed scheme showed the best performance. Since there was no significant difference in the average PDR between the two MB-ADR schemes in this subset, this metric was not further analyzed.

As shown in Figure 4(a), the enhanced MB-ADR demonstrates a significant advantage in average energy efficiency compared to the other schemes in instances with fewer EDs. As the number of devices increases, the MB-ADR schemes tend to converge, but the dynamic scheme still maintains the best performance, showing an overall improvement of approximately 52.5% and 107% compared to the original MB-ADR and standard ADR, respectively.

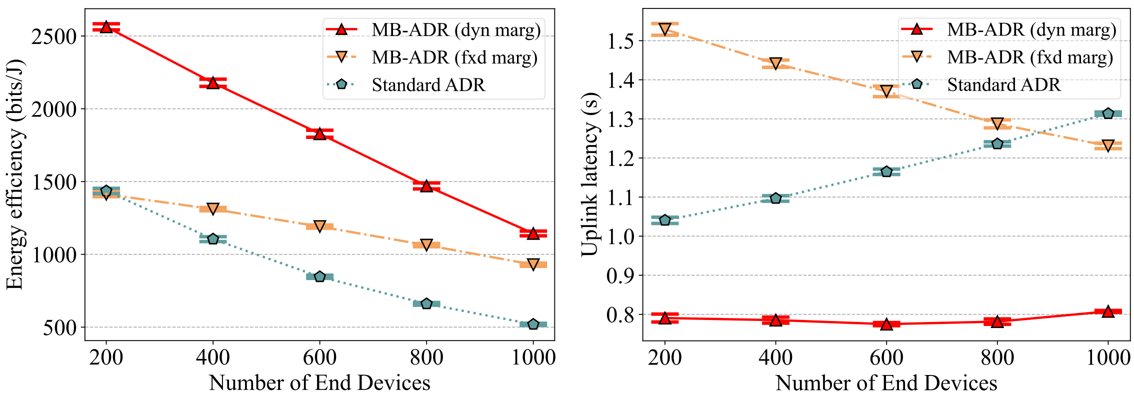


(a) (b)

**Figure 4. Network performance for varying numbers of end devices in terms of average (a) energy efficiency and (b) uplink latency.**

In the same speed range, regarding latency, the enhanced MB-ADR consistently achieves lower average delays compared to the other schemes, as illustrated in Figure 4(b).

In this analysis, the enhanced MB-ADR achieves an overall improvement of approximately 42.18% and 32.23% compared to the original MB-ADR and standard ADR, respectively.

Analyzing the final SF assignment reveals the cause-and-effect relationship in each scheme's performance. For the first speed class, shown in Figure 5(a), the enhanced MB-ADR allocates more SF7 and fewer SF12 instances than the original MB-ADR. While this increases packet loss due to lower sensitivity, it reduces energy consumption. In contrast, standard ADR focuses more on SF7, resulting in low energy consumption but excessive packet loss, which consequently affects its energy efficiency.

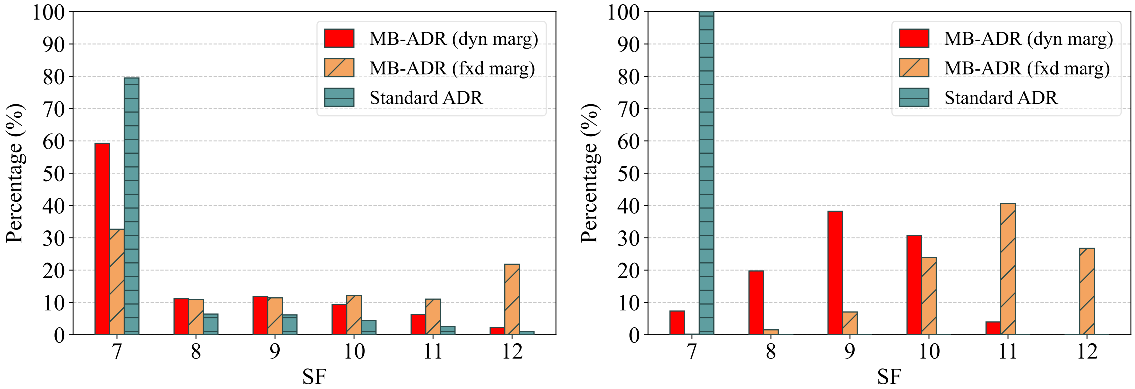


(a) (b)

**Figure 5. Final SF assignment for the speed classes: (a) [0.1, 4] m/s and (b) [16, 20] m/s.**

Conversely, for the last speed class, as shown in Figure 5(b), the standard ADR exhibits a more imbalanced SF distribution, explaining the significant performance degradation. This aligns with expectations for schemes unsuitable for mobility. The enhanced MB-ADR, however, shows a more balanced SF distribution with a tendency for lower SF values, reducing modulation overhead and improving energy efficiency and latency compared to the original MB-ADR.

Analysis indicates that using a fixed $margin\_db$ value can result in unnecessarily high SF values. In mobility scenarios, the enhanced MB-ADR achieved a comparable PDR to the fixed-margin MB-ADR while significantly improving energy efficiency and latency due to dynamic adjustment of $margin\_db$ to match changing channel conditions.

## 7. Conclusion

The enhanced MB-ADR algorithm presented in this study addresses the limitations of existing ADR mechanisms for LoRaWAN in mobile environments. By dynamically adjusting the variable $margin\_db$ based on SNR variability, the proposed scheme improves energy efficiency and latency without compromising packet delivery, especially in high-mobility scenarios. The enhanced MB-ADR achieved an overall improvement of 52.5% and 107% in energy efficiency compared to the original MB-ADR and standard ADR, respectively, demonstrating the adaptability and robustness of the dynamic margin approach.

Future work may integrate this scheme with predictive models for improved parameter adaptation in dynamic networks, explore scalability in ultra-dense IoT environments, and assess performance in multi-gateway architectures. Combining dynamic ADR with machine learning could further enhance energy efficiency and network reliability, helping LoRaWAN meet the evolving demands of IoT ecosystems.

## References


Al-Gumaei, Y. A., Aslam, N., Aljaidi, M., Al-Saman, A., Alsarhan, A., and Ashyap, A. Y. (2022). A Novel Approach to Improve the Adaptive-Data-Rate Scheme for IoT LoRaWAN. *Electronics*, 11(21).

Anwar, K., Rahman, T., Zeb, A., Khan, I., Zareei, M., and Vargas-Rosales, C. (2021). RM-ADR: Resource Management Adaptive Data Rate for Mobile Application in LoRaWAN. *Sensors*, 21(23).

Benkahla, N., Tounsi, H., Song, Y.-Q., and Frikha, M. (2021). VHMM-based E-ADR for LoRaWAN networks with unknown mobility patterns. In *2021 International Wireless Communications and Mobile Computing (IWCMC)*, pages 86–91.

Bonilla, V., Campoverde, B., and Yoo, S. G. (2023). A Systematic Literature Review of LoRaWAN: Sensors and Applications. *Sensors*, 23(20).

de Jesus, G. G. M., Souza, R. D., Montez, C., and Hoeller, A. (2021). LoRaWAN Adaptive Data Rate With Flexible Link Margin. *IEEE Internet of Things Journal*, 8(7):6053–6061.

Di Renzone, G., Parrino, S., Peruzzi, G., Pozzebon, A., and Vangelista, L. (2024). Lorawan for vehicular networking: Field tests for vehicle-to-roadside communication. *Sensors*, 24(6).

Duan, B., Li, C., Xie, J., Wu, W., and Zhou, D. (2021). Fast Handover Algorithm Based on Location and Weight in 5G-R Wireless Communications for High-Speed Railways. *Sensors*, 21(9).

Durand, A., El Rachkidy, N., and Guitton, A. (2023). MADERE: Mobile Adaptive Datarate for LoRaWAN. In *2023 IEEE Wireless Communications and Networking Conference (WCNC)*, pages 1–6.

El Chall, R., Lahoud, S., and El Helou, M. (2019). Lorawan network: Radio propagation models and performance evaluation in various environments in lebanon. *IEEE Internet of Things Journal*, 6(2):2366–2378.

Farhad, A., Kwon, G.-R., and Pyun, J.-Y. (2023). Mobility Adaptive Data Rate Based on Kalman Filter for LoRa-Empowered IoT Applications. In *2023 IEEE 20th Consumer Communications & Networking Conference (CCNC)*, pages 321–324.

Ferrari, P., Sisinni, E., Carvalho, D. F., Depari, A., Signoretti, G., Silva, M., Silva, I., and Silva, D. (2020). On the use of lorawan for the internet of intelligent vehicles in smart city scenarios. In *2020 IEEE Sensors Applications Symposium (SAS)*, pages 1–6.

Janssen, T., Koppert, A., Berkvens, R., and Weyn, M. (2023). A Survey on IoT Positioning Leveraging LPWAN, GNSS, and LEO-PNT. *IEEE Internet of Things Journal*, 10(13):11135–11159.

Jiang, Y., Wang, M., and Wang, X. (2023). A Efficient Adaptive Data Rate Algorithm in LoRaWAN Networks: K-ADR. In *2023 24st Asia-Pacific Network Operations and Management Symposium (APNOMS)*, pages 183–188.

Kufakunesu, R., Hancke, G., and Abu-Mahfouz, A. (2022). A Fuzzy-Logic Based Adaptive Data Rate Scheme for Energy-Efficient LoRaWAN Communication. *Journal of Sensor and Actuator Networks*, 11:65.

Kufakunesu, R., Hancke, G. P., and Abu-Mahfouz, A. M. (2020). A Survey on Adaptive Data Rate Optimization in LoRaWAN: Recent Solutions and Major Challenges. *Sensors*, 20(18).

Moysiadis, V., Lagkas, T., Argyriou, V., Sarigiannidis, A., Moscholios, I. D., and Sarigiannidis, P. (2021). Extending ADR mechanism for LoRa enabled mobile end-devices. *Simulation Modelling Practice and Theory*, 113:102388.

Nico, V. and Punch, J. (2019). Two-degree-of-freedom velocity-amplified vibrational energy harvester for human motion applications. *The European Physical Journal Special Topics*, 228(7):1647–1657.

Ouermi, T. A. J., Li, J., Athawale, T. M., and Johnson, C. R. (2024). Estimation and Visualization of Isosurface Uncertainty from Linear and High-Order Interpolation Methods. In *2024 IEEE Workshop on Uncertainty Visualization: Applications, Techniques, Software, and Decision Frameworks*, pages 51–61.

Perez, H. and Tah, J. H. M. (2020). Improving the Accuracy of Convolutional Neural Networks by Identifying and Removing Outlier Images in Datasets Using t-SNE. *Mathematics*, 8(5).

Ren, Y., Liu, L., Li, C., Cao, Z., and Chen, S. (2022). Is lorawan really wide? fine-grained lora link-level measurement in an urban environment. In *2022 IEEE 30th International Conference on Network Protocols (ICNP)*, pages 1–12.

Sarmento Neto, G. A., Da Silva, T. A. R., Abreu, P. F. F., Veloso, A. F. D. S., Mendes, L. H. d. O., and Dos Reis, J. V. (2024). Addressing Mobility Challenges in LoRaWAN through Adaptive Data Rate: A Statistical Median-Based Approach. In *2024 11th International Conference on Future Internet of Things and Cloud (FiCloud)*, pages 330–337.

Semtech (2016). LoRaWAN Simple Rate Adaptation Recommended Algorithm. Rev. 1.0. `https://bit.ly/40m8DKA`. Retrieved on January 6, 2025.

Soy, H. (2023). An adaptive spreading factor allocation scheme for mobile LoRa networks: Blind ADR with distributed TDMA scheduling. *Simulation Modelling Practice and Theory*, 125:102755.

Teymuri, B., Serati, R., Anagnostopoulos, N. A., and Rasti, M. (2023). Lp-mab: Improving the energy efficiency of lorawan using a reinforcement-learning-based adaptive configuration algorithm. *Sensors*, 23(4).

Wang, H., Zhang, X., Liao, J., Zhang, Y., and Li, H. (2024). An improved adaptive data rate algorithm of LoRaWAN for agricultural mobile sensor nodes. *Computers and Electronics in Agriculture*, 219:108773.